

STELLAR EVIDENCE THAT THE SOLAR DYNAMO MAY BE IN TRANSITION

TRAVIS S. METCALFE^{1,2}, RICKY EGELAND^{3,4}, JENNIFER VAN SADERS^{5,6}

¹Space Science Institute, 4750 Walnut St. Suite 205, Boulder CO 80301 USA

²Visiting Scientist, National Solar Observatory, 3665 Discovery Dr., Boulder CO 80303 USA

³High Altitude Observatory, National Center for Atmospheric Research, P.O. Box 3000, Boulder CO 80307 USA

⁴Department of Physics, Montana State University, Bozeman MT 59717 USA

⁵Carnegie Observatories, 813 Santa Barbara St, Pasadena CA 91101 USA

⁶Department of Astrophysical Sciences, Princeton University, Princeton NJ 08544 USA

ABSTRACT

Precise photometry from the *Kepler* space telescope allows not only the measurement of rotation in solar-type field stars, but also the determination of reliable masses and ages from asteroseismology. These critical data have recently provided the first opportunity to calibrate rotation-age relations for stars older than the Sun. The evolutionary picture that emerges is surprising: beyond middle-age the efficiency of magnetic braking is dramatically reduced, implying a fundamental change in angular momentum loss beyond a critical Rossby number ($\text{Ro} \sim 2$). We compile published chromospheric activity measurements for the sample of *Kepler* asteroseismic targets that were used to establish the new rotation-age relations. We use these data along with a sample of well-characterized solar analogs from the Mount Wilson HK survey to develop a qualitative scenario connecting the evolution of chromospheric activity to a fundamental shift in the character of differential rotation. We conclude that the Sun may be in a transitional evolutionary phase, and that its magnetic cycle might represent a special case of stellar dynamo theory.

Keywords: stars: activity—stars: evolution—stars: magnetic field—stars: rotation—stars: solar-type

1. INTRODUCTION

One of the biggest surprises from the *Kepler* space telescope is that there were so few surprises for stars near the main-sequence. Stellar evolution models that had been calibrated to match the properties of the Sun were generally sufficient to reproduce asteroseismic observations of other solar-type stars. For example, [Metcalf et al. \(2015\)](#) used a solar data set comparable to what *Kepler* obtained for other solar-type stars and recovered the solar age and other properties with an absolute accuracy better than 5%. Identical methods applied independently to the complete *Kepler* data sets for 16 Cyg A & B found the same age and composition for the two components, bolstering our confidence in the reliability of asteroseismic techniques.

A major surprise for *Kepler* main-sequence stars arose when asteroseismic properties were confronted with measurements of rotation. The idea of using rotation as a diagnostic of stellar age dates back to [Skumanich \(1972\)](#), and decades of effort have gone into calibrating the modern concept of *gyrochronology* ([Barnes 2007](#)). The initial contributions from *Kepler* included observations of stellar rotation in the 1 Gyr-old cluster

NGC 6811 ([Meibom et al. 2011](#)) and the 2.5 Gyr-old cluster NGC 6819 ([Meibom et al. 2015](#)), extending the calibration of the method significantly beyond previous work. Initial indications of a possible conflict between asteroseismology and gyrochronology were noted by [Angus et al. \(2015\)](#), who found that no single color-dependent relationship between rotation and age could simultaneously describe the cluster and field populations. Although they used low-precision asteroseismic ages from grid-based modeling ([Chaplin et al. 2014](#)), the tension was still evident.

The source of disagreement between the age scales from asteroseismology and gyrochronology came into focus after [van Saders et al. \(2016\)](#) scrutinized *Kepler* targets with precise ages from detailed modeling. They confirmed the existence of a population of field stars rotating more quickly than expected from gyrochronology. They discovered that the anomalous rotation became significant near the solar age for G-type targets, but it appeared earlier in F-type stars and later in K-type stars. This dependence on spectral type suggested a connection to the Rossby number ($\text{Ro} \equiv P_{\text{rot}}/\tau_c$), the ratio of the rotation period to the convective turnover

Table 1. Properties of the asteroseismic sample with rotation and activity data.

KIC	$B-V$	R/R_{\odot}	M/M_{\odot}	t/Gyr	P_{rot}	$\log R'_{HK}$	Sources
3656476	0.782	1.335 ± 0.009	1.13 ± 0.03	8.67 ± 0.61	31.67 ± 3.53	-5.109	1,6,11
5184732	0.696	1.367 ± 0.013	1.27 ± 0.04	4.17 ± 0.39	19.79 ± 2.43	-5.130	1,6,8
6116048	0.589	1.219 ± 0.009	1.01 ± 0.03	6.23 ± 0.37	17.26 ± 1.96	-5.019	2,6,9
6521045	0.790	1.474 ± 0.013	1.04 ± 0.02	6.24 ± 0.64	25.34 ± 2.78	-5.042	4,4,10
7680114	0.690	1.421 ± 0.012	1.12 ± 0.03	7.35 ± 0.78	26.31 ± 1.86	-4.905	1,6,11
8006161	0.859	0.947 ± 0.007	1.04 ± 0.02	5.04 ± 0.17	29.79 ± 3.09	-5.011	2,6,9
8379927	0.570	1.130 ± 0.013	1.15 ± 0.04	1.67 ± 0.12	16.99 ± 1.35	-4.834	5,6,9
9098294	0.567	1.154 ± 0.009	1.00 ± 0.03	7.28 ± 0.51	19.79 ± 1.33	-5.020	2,6,9
9139151	0.520	1.146 ± 0.011	1.14 ± 0.03	1.71 ± 0.19	10.96 ± 2.22	-4.954	2,6,9
9955598	0.713	0.907 ± 0.005	0.96 ± 0.03	6.43 ± 0.40	34.20 ± 5.64	-5.048	4,6,10
10454113	0.528	1.250 ± 0.015	1.19 ± 0.04	2.03 ± 0.29	14.61 ± 1.09	-4.872	2,6,9
10644253	0.598	1.108 ± 0.016	1.13 ± 0.05	1.07 ± 0.25	10.91 ± 0.87	-4.696	2,6,11
10963065	0.509	1.222 ± 0.010	1.07 ± 0.03	4.36 ± 0.29	12.58 ± 1.70	-5.054	4,6,10
11244118	0.732	1.589 ± 0.026	1.10 ± 0.05	6.43 ± 0.58	23.17 ± 3.89	-5.148	2,6,9
12009504	0.556	1.375 ± 0.015	1.12 ± 0.03	3.64 ± 0.26	9.39 ± 0.68	-4.977	2,6,9
12069424	0.643	1.236 ± 0.008	1.10 ± 0.02	7.07 ± 0.46	$23.8^{+1.5}_{-1.8}$	-5.105	3,3,7
12069449	0.661	1.123 ± 0.007	1.06 ± 0.02	6.82 ± 0.28	$23.2^{+11.5}_{-3.2}$	-5.094	3,3,7
12258514	0.599	1.573 ± 0.010	1.19 ± 0.03	4.03 ± 0.32	15.00 ± 1.84	-5.024	2,5,9

References—(1) [Mathur et al. \(2012\)](#); (2) [Metcalf et al. \(2014\)](#); (3) [Davies et al. \(2015\)](#); (4) [Ceillier et al. \(2016\)](#); (5) [Davies et al. \(in preparation\)](#); (6) [García et al. \(2014\)](#); (7) [Wright et al. \(2004\)](#); (8) [Isaacson & Fischer \(2010\)](#); (9) [Karoff et al. \(2013\)](#); (10) [Marcy et al. \(2014\)](#); (11) [Salabert et al. \(2016\)](#)

time. They proposed that magnetic braking operates with a dramatically reduced efficiency beyond a critical Rossby number, and they reproduced the observations with rotational evolution models that eliminated angular momentum loss beyond $\text{Ro} \sim 2$.

Motivated by these results, we search for a magnetic counterpart to the rotational transition discovered by [van Saders et al. \(2016\)](#). We compile published chromospheric activity measurements for the *Kepler* sample, and we compare them to a selection of G-type stars from the Mount Wilson HK survey ([Baliunas et al. 1996](#); [Donahue et al. 1996](#)). We use these observations to reinterpret some well-established features of chromospheric activity in solar-type stars, and we propose a qualitative scenario for magnetic evolution that connects the available evidence to a shift in the character of differential rotation (section 2). We then use a sample of well-characterized solar analogs to constrain the evolution of key dynamo ingredients and outputs (section 3), with a particular focus on the magnetic topology revealed by Zeeman Doppler imaging (ZDI, [Petit et al. 2008](#)). We conclude that the Sun may be in a transitional evolutionary phase, and we discuss the implications for understanding the solar magnetic cycle in the context of activity cycles observed in other stars (section 4).

2. ROTATION-ACTIVITY RELATION

We have identified chromospheric activity measurements for 18 of the 21 stars in the [van Saders et al. \(2016\)](#) sample, which are listed with their asteroseismic properties and rotation periods in Table 1. All of the asteroseismic data were analyzed using the method described in [Metcalf et al. \(2014\)](#), and most of the rotation periods were obtained from the method described in [García et al. \(2014\)](#). The activity data come from multiple sources, but we gave priority to measurements made by [Karoff et al. \(2013\)](#) during the *Kepler* mission.

Our sample is dominated by stars more evolved than the Sun because of two selection effects. First, the intrinsic amplitudes of solar-like oscillations scale with the ratio of luminosity to mass ([Houdek et al. 1999](#); [Samadi & Goupil 2001](#)), making them easier to detect in early-type and more evolved stars. Second, the observed amplitudes are suppressed by strong magnetic activity ([Chaplin et al. 2011](#)), biasing detections away from young main-sequence stars. Consequently, the youngest and most active targets in our sample are F-type stars.

The relationship between chromospheric activity and rotation for our sample is illustrated in Figure 1 with colored points, including F-type (blue triangles), G-type (orange circles), and K-type (red squares) targets. For

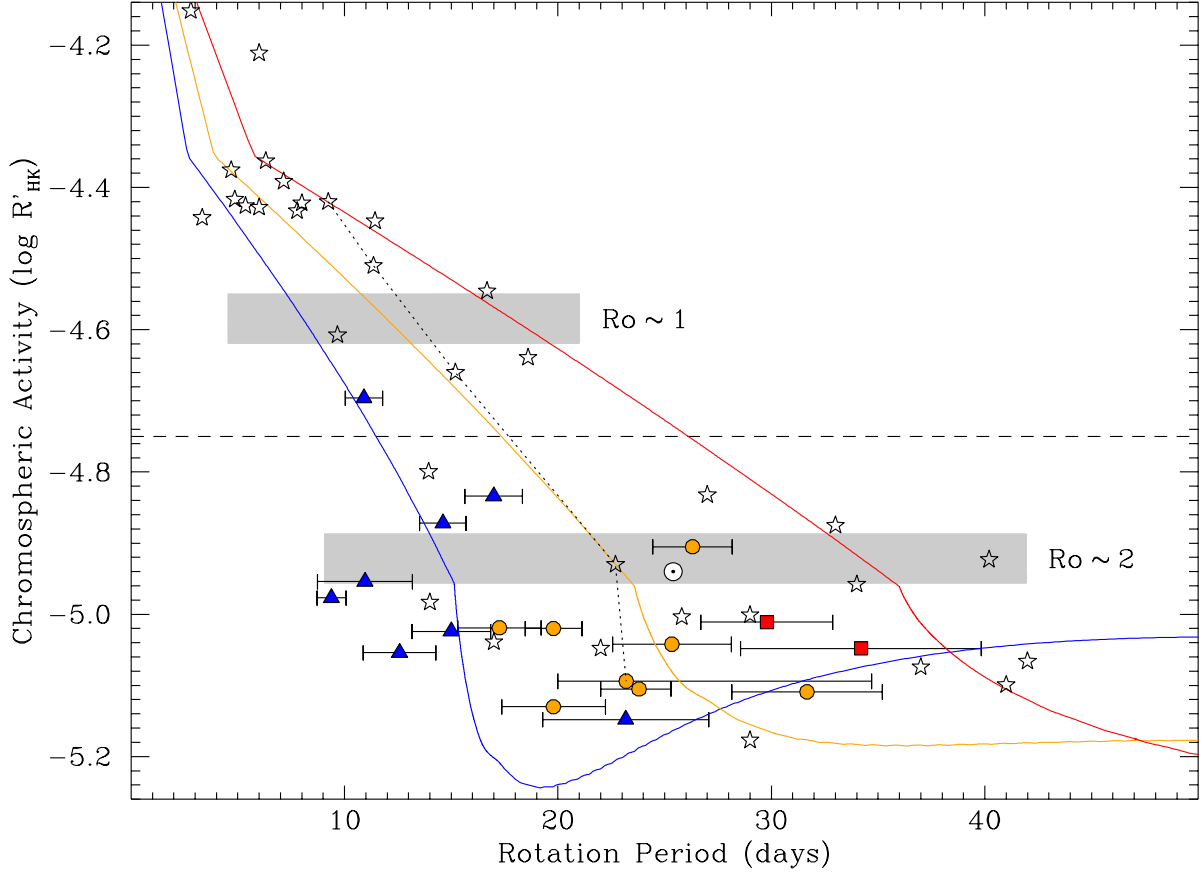


Figure 1. Relationship between chromospheric activity and rotation in field dwarfs and subgiants. G-type stars from the Mount Wilson HK project are shown as star symbols. The asteroseismic sample from *Kepler* is shown as colored points, including F-type (blue triangles), G-type (orange circles), and K-type (red squares) stars. The Sun is shown with its usual symbol (\odot). The dashed line indicates the activity level of the Vaughan-Preston gap while the dotted line connects several well-characterized solar analogs. Shaded regions denote the activity levels that correspond to key Rossby numbers, using the empirical activity-rotation relation from Mamajek & Hillenbrand (2008). Colored curves use this same relation to plot rotational evolution models from van Saders et al. (2016) for KIC 10963065 (blue), KIC 6521045 (orange), and KIC 9955598 (red).

context, we also show a selection of G-type stars from the Mount Wilson HK survey (star symbols) and a few rotational evolution models from van Saders et al. (2016), converted from Rossby number to chromospheric activity using the rotation-activity relation of Mamajek & Hillenbrand (2008). We extrapolate this relation for $\log R'_{\text{HK}} < -5.0$, where the evolution tracks exceed a critical Rossby number ($\text{Ro}_{\text{crit}} = 2.1$) and magnetic braking ceases. The activity levels that correspond to key Rossby numbers are shown as shaded regions on either side of the Vaughan-Preston gap (dashed line, Vaughan & Preston 1980). The vertical extent of the shaded regions indicates the variation of solar activity through a magnetic cycle (Hall & Lockwood 2004), while the horizontal extent corresponds to the variation in convective turnover times for the color range of our sample. The dotted line connects several well-characterized solar analogs (see section 3).

The horizontal spread in rotation rates at low activity levels is evident both in our sample and in the Mount

Wilson stars. This can largely be understood as a consequence of how the convective turnover time depends on spectral type, such that stars with deeper convection zones spend more time at a given activity level. At the lowest activity levels the evolution changes abruptly, leading to an excess of evolved stars with relatively short rotation periods. This can most easily be seen for the F-type and G-type stars, with rotation periods around 10 and 20 days respectively.

As suggested by van Saders et al. (2016), one way to reduce the efficiency of magnetic braking is to concentrate the field into smaller spatial scales. For example, Réville et al. (2015) demonstrated that the dipole component of the field is responsible for most of the angular momentum loss due to the magnetized stellar wind. *We propose that a change in the character of differential rotation is the underlying mechanism that ultimately disrupts the large-scale organization of magnetic field in solar-type stars.* The process begins at $\text{Ro} \sim 1$, where the rotation period becomes comparable to the convec-

Table 2. Properties of the solar analog sample.

	HD 20630	HD 30495	HD 76151	18 Sco	16 Cyg B
Spectral Type	G5V	G1.5V	G3V	G2V	G3V
R/R_{\odot}	0.917 ± 0.011	0.983 ± 0.016	0.979 ± 0.017	1.010 ± 0.009	1.116 ± 0.006
M/M_{\odot}	0.95 ± 0.09	0.86 ± 0.12	1.24 ± 0.12	1.03 ± 0.01	1.04 ± 0.02
Age [Gyr]	0.5 ± 0.1	1.0 ± 0.1	1.4 ± 0.2	$3.66^{+0.44}_{-0.50}$	6.74 ± 0.24
P_{rot} [d]	9.24	11.36	15.2	22.7	23.2
$\Delta P/P$	0.0509	0.0519
Ro	0.70	1.08	1.18	1.92	2.10
$\log R'_{\text{HK}}$	-4.42	-4.51	-4.66	-4.93	-5.09
$P_{\text{cyc}}(\text{A})$ [yr]	5.6	12.2
$P_{\text{cyc}}(\text{I})$ [yr]	...	1.67	2.52	7.1	...
Sources	1,5,7,11,14	1,6,11	1,5,8,11,14	2,4,9,12	3,10,13

References—(1) [Valenti & Fischer \(2005\)](#); (2) [Bazot et al. \(2011\)](#); (3) [Metcalf et al. \(2015\)](#); (4) [Li et al. \(2012\)](#); (5) [Barnes \(2007\)](#); (6) [Egeland et al. \(2015\)](#); (7) [Donahue et al. \(1996\)](#); (8) [Oláh et al. \(2016\)](#); (9) [Petit et al. \(2008\)](#); (10) [Davies et al. \(2015\)](#); (11) [Baliunas et al. \(1996\)](#); (12) [Hall et al. \(2007a\)](#); (13) [Wright et al. \(2004\)](#); (14) [Baliunas et al. \(1995\)](#)

tive turnover time. Differential rotation is an emergent property of turbulent convection in the presence of Coriolis forces, and [Gastine et al. \(2014\)](#) showed that many global convection simulations exhibit a transition from solar-like to anti-solar differential rotation near $\text{Ro} \sim 1$.

We can then interpret the Vaughan-Preston gap as a signature of rapid magnetic evolution triggered by a shift in the character of differential rotation. [Pace et al. \(2009\)](#) used activity measurements of stars in several open clusters to constrain the age of F-type stars crossing the gap to be between 1.2 and 1.4 Gyr. The two most active F-type stars in our sample have ages of 1.07 and 1.67 Gyr and fall on opposite sides of the gap, consistent with the results of [Pace et al. \(2009\)](#) and validating our asteroseismic age scale.

According to [Lockwood et al. \(2007\)](#), the Vaughan-Preston gap also corresponds to a shift from spots to faculae as the dominant source of photometric variability on the timescale of stellar cycles. [Shapiro et al. \(2014\)](#) noted that the surface area of spots varies quadratically with activity level over the solar cycle, while faculae vary linearly. Extrapolating to higher activity levels they reproduced the transition from spot- to faculae-dominated variability across the Vaughan-Preston gap. They do not offer an explanation for the quadratic dependence of spot area on activity level in the Sun. We speculate that an accelerated decrease in the surface area of spots may be one consequence of a disruption of differential rotation at $\text{Ro} \sim 1$.

Emerging from the rapid magnetic evolution across the Vaughan-Preston gap, stars reach the $\text{Ro} \sim 2$ threshold where magnetic braking operates with a dramati-

cally reduced efficiency, possibly due to a shift in magnetic topology (see section 3). The rotation period then evolves as the star undergoes slow expansion and changes its moment of inertia as it ages. At the same time, the activity level decreases with effective temperature as the star expands and mechanical energy from convection largely replaces magnetic energy driven by rotation as the dominant source of chromospheric heating ([Böhm-Vitense 2007](#)).

3. EVIDENCE FROM SOLAR ANALOGS

Although the basic stellar properties of the *Kepler* sample are well-constrained from asteroseismology, characterization of their magnetic cycles and differential rotation will require additional observations and analysis. In the meantime, we use a selection of well-characterized solar analogs to investigate the evolution of key dynamo ingredients and outputs for solar-type stars as they pass through various stages of the scenario outlined in section 2. These solar analogs are connected with a dotted line in Figure 1, their properties are listed in Table 2, and we discuss them below from high to low activity.

The most active of our selected solar analogs is HD 20630 (κ^1 Cet), which has not yet experienced a putative shift in the character of differential rotation at $\text{Ro} \sim 1$. [Walker et al. \(2007\)](#) modeled three seasons of photometry from the MOST satellite to establish that HD 20630 shows solar-like differential rotation, as expected. The latitudinal shear is slightly smaller than in the Sun, but the modeled spots appear over a wide range of active latitudes from 10° to 75° . [Baliunas et al. \(1995\)](#) identified a 5.6 year cycle in the chromospheric activity. For a rotation period of 9.24 d ([Donahue et al.](#)

1996), this is a normal cycle on the active (A) branch (Saar & Brandenburg 1999; Böhm-Vitense 2007).

Slightly closer to the $Ro \sim 1$ transition is HD 30495, which was recently characterized by Egeland et al. (2015) from 47 years of activity measurements and 22 years of photometry. The average rotation period of 11.36 d varied between seasons, suggesting a broad range of active latitudes and implying a surface shear less than or comparable to the Sun. The unknown latitudes of the spots prevented the authors from determining the sense of the differential rotation. However, the brightness variations were unambiguously dominated by spots rather than faculae, as expected for a star on the active side of the Vaughan-Preston gap. They identified magnetic variability on two different timescales, with an average long cycle of 12.2 years and persistent short-term variability around 1.67 years. These periods are comparable to the sunspot cycle and quasi-biennial variations (Bazilevskaya et al. 2014) but in a star rotating at more than twice the rate of the Sun. The long cycle falls squarely on the A-branch, while the short-period variations can be interpreted as a secondary cycle on the inactive (I) branch (Saar & Brandenburg 1999; Böhm-Vitense 2007).

Just above the activity level of the Vaughan-Preston gap is HD 76151, one of the solar analogs observed with ZDI by Petit et al. (2008). The equatorial rotation period inferred from spectropolarimetry (20.5 d) is significantly longer than that determined from chromospheric activity measurements (15.2 d, Oláh et al. 2016), which reflects rotation at the active latitudes. If both periods are reliable, it implies strong anti-solar differential rotation in this star. Petit et al. (2008) found no indication of surface differential rotation, but they only made such a detection for the most active star in their sample. However, they found that 93% of the magnetic energy in HD 76151 was in the poloidal component of the field. More generally, they found that a growing fraction of the field was poloidal in solar analogs as rotation slowed. In flux-transport dynamo models, differential rotation is the mechanism that recycles poloidal field into the toroidal component (e.g., Dikpati & Gilman 2009), so this trend can be interpreted as evidence of inefficient differential rotation. Decomposing the poloidal field into spherical harmonics, they found 79% in the dipole component and 18% in the quadrupole. HD 76151 has the shortest activity cycle reported by the Mount Wilson HK survey (2.52 years, Baliunas et al. 1995), which falls on the I-branch.

On the opposite side of the Vaughan-Preston gap near $Ro \sim 2$ is the well-known solar twin HD 146233 (18 Sco). As expected, Hall et al. (2007b) found the brightness variations to be dominated by faculae just as in the Sun. Petit et al. (2008) found more than 99% of the magnetic

energy concentrated in poloidal field, a further indication of the diminishing role of differential rotation. Most interesting from the standpoint of weakened magnetic braking, only 34% of the poloidal field was in the dipole component while 56% was in the quadrupole. The ZDI measurements were obtained near a maximum in magnetic activity, so we might expect this solar twin to be dominated by the quadrupole. Indeed, a low-order reconstruction of the solar magnetic field near maximum by Vidotto (2016) resembles the ZDI map of 18 Sco. Hall et al. (2007b) identified a 7 year activity cycle in 18 Sco, which appears to be a normal cycle on the I-branch unlike the 11 year solar cycle.

Beyond the transition to reduced magnetic braking is the solar analog binary 16 Cyg A & B, which is also part of our *Kepler* sample. García et al. (2014) found no significant photometric variation, so the rotation periods were determined by Davies et al. (2015) from frequency splitting of the oscillation modes. For a sample of *Kepler* targets that also showed spot modulations, Nielsen et al. (2015) demonstrated that the two methods yield consistent results. They also noted an absence of significant radial differential rotation in their sample, providing further evidence of minimal shear at these low activity levels. Despite an impressive signal-to-noise ratio, P. Petit (priv. comm.) found no detectable Zeeman signatures in spectropolarimetry of 16 Cyg A & B. If present, the dipole component would be the easiest signal to detect. Chromospheric activity monitoring from Lowell Observatory since 1994 (Hall et al. 2007a) shows both components with activity levels below that of the Sun at solar minimum, and no cyclic variation.

4. CONCLUSIONS & DISCUSSION

Based on the scenario for magnetic evolution outlined in section 2 and considering the evidence from solar analogs presented in section 3, we conclude that the Sun may be in a transitional evolutionary phase and that it might represent a special case of stellar dynamo theory. The Sun obviously exhibits solar-like differential rotation, so the transition at $Ro \sim 1$ suggested by simulations may be more complex than a shift to anti-solar latitudinal shear. The Sun appears to have a narrower range of active latitudes than the most active solar analogs, and the torsional oscillations observed from helioseismology (Vorontsov et al. 2002) may be one indication of an ongoing transition in the character of differential rotation. The concentration of magnetic energy into poloidal field for solar analogs that span the Vaughan-Preston gap is further evidence of relatively inefficient differential rotation. The Sun still exhibits a dipole component to its global field, particularly near magnetic minimum, but the solar analogs also suggest a gradual concentration of the field into smaller spatial scales, leading to weakened

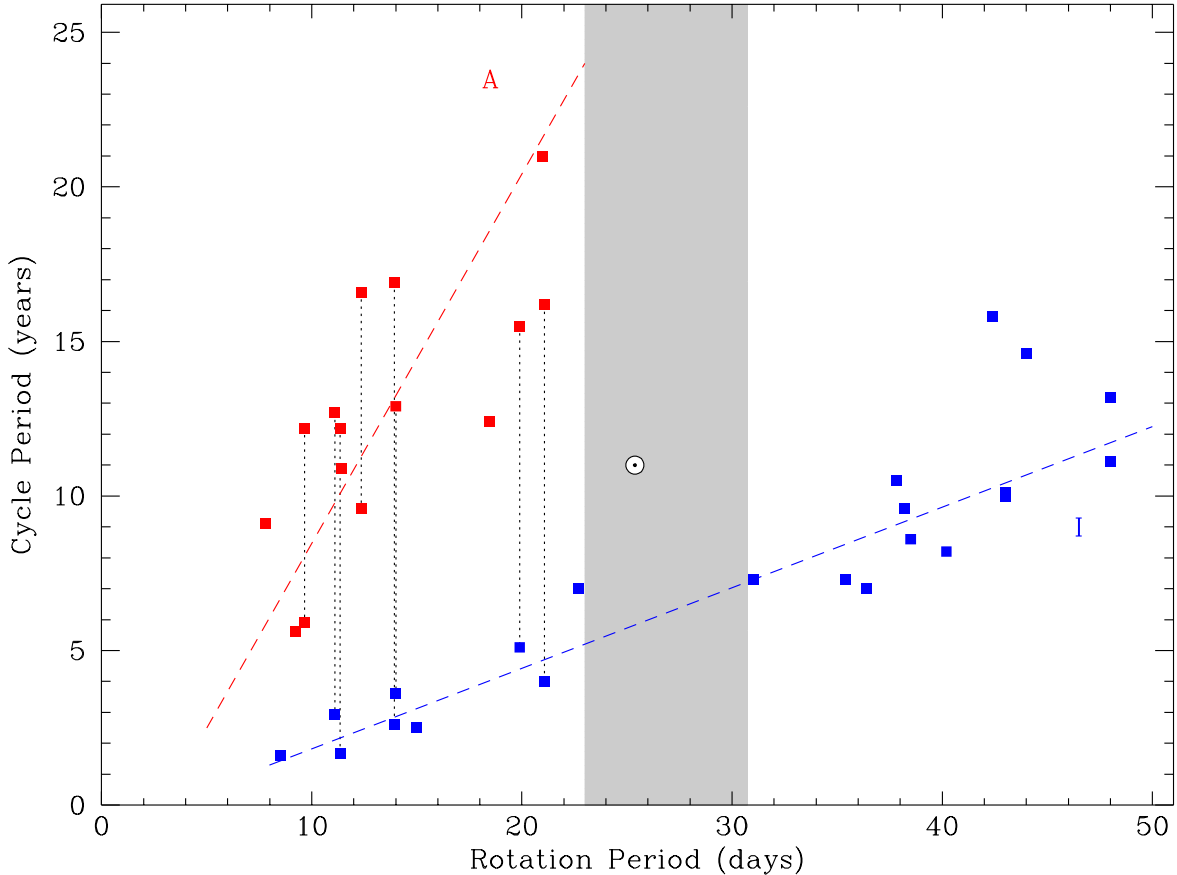


Figure 2. Updated version of a diagram published in [Böhm-Vitense \(2007\)](#) using data from [Saar & Brandenburg \(1999\)](#), showing the active (A) and inactive (I) branches. More recent data have been added from [Hall et al. \(2007b\)](#), [Metcalf et al. \(2010, 2013\)](#), and [Egeland et al. \(2015\)](#). Multiple cycles observed in the same star are connected with vertical dotted lines. The shaded region indicates the range of rotation periods around the Sun (\odot) where the Mount Wilson targets are flat-activity stars.

magnetic braking. Such a transition may represent the shift from a dominant α - Ω dynamo to an α^2 dynamo, but this remains to be demonstrated.

Perhaps the most significant indication that the Sun is in a transitional evolutionary phase is its 11 year magnetic cycle, which falls between the active and inactive branches established by other stars (see Figure 2). Even the slightly younger solar twin 18 Sco exhibits a normal cycle on the I-branch, while the Sun is the only star with a rotation period between 23-30 d that shows a cycle at all. There were several Mount Wilson targets with rotation periods in this range, but they are all flat-activity stars. The Maunder minimum may represent one manifestation of the Sun beginning to enter this flat-activity phase. The fact that all of the slower rotators with cycles are K-type stars is perfectly understandable, since magnetic braking ceases in G-type stars before they reach these long rotation periods. Among the faster rotators, many of the Mount Wilson targets appeared to have chaotic variability in their chromospheric activity. This may be due to the ubiquity of secondary cycles on the I-branch, combined with seasonal data gaps that fail to sample these short periods adequately.

Future observations and analysis will offer additional tests of the scenario for magnetic evolution described in section 2. The sample of *Kepler* targets with asteroseismic ages and detected rotation periods promises to expand to ~ 30 stars from analysis of the full-length data sets (Lund et al. in preparation). Only a few of these targets have not yet made the transition to weakened magnetic braking, so further characterization of the bright solar analogs will be essential to establish the nature and timing of the chain of events that lead to this evolutionary phase. Additional ZDI measurements of solar analogs, more constraints on differential rotation at various activity levels, and asteroseismic observations of Mount Wilson stars with the K2 and TESS missions will all be helpful.

The authors would like to thank Axel Brandenburg, Paul Charbonneau, Mark Giampapa, Peter Gilman, Marc Pinsonneault, Steve Saar, Dave Soderblom and Ellen Zweibel for helpful discussions. This work was supported in part by NASA grant NNX15AF13G. R. E. is supported by a Newkirk Fellowship at the High Altitude Observatory.

REFERENCES

- Angus, R., Aigrain, S., Foreman-Mackey, D., & McQuillan, A. 2015, *MNRAS*, 450, 1787
- Baliunas, S. L., Donahue, R. A., Soon, W. H., et al. 1995, *ApJ*, 438, 269
- Baliunas, S., Sokoloff, D., & Soon, W. 1996, *ApJL*, 457, L99
- Barnes, S. A. 2007, *ApJ*, 669, 1167
- Bazilevskaya, G., Broomhall, A.-M., Elsworth, Y., & Nakariakov, V. M. 2014, *SSRv*, 186, 359
- Bazot, M., Ireland, M. J., Huber, D., et al. 2011, *A&A*, 526, L4
- Böhm-Vitense, E. 2007, *ApJ*, 657, 486
- Ceillier, T., van Saders, J., García, R. A., et al. 2016, *MNRAS*, 456, 119
- Chaplin, W. J., Bedding, T. R., Bonanno, A., et al. 2011, *ApJL*, 732, L5
- Chaplin, W. J., Basu, S., Huber, D., et al. 2014, *ApJS*, 210, 1
- Davies, G. R., Chaplin, W. J., Farr, W. M., et al. 2015, *MNRAS*, 446, 2959
- Dikpati, M., & Gilman, P. A. 2009, *SSRv*, 144, 67
- Donahue, R. A., Saar, S. H., & Baliunas, S. L. 1996, *ApJ*, 466, 384
- Egeland, R., Metcalfe, T. S., Hall, J. C., & Henry, G. W. 2015, *ApJ*, 812, 12
- García, R. A., Ceillier, T., Salabert, D., et al. 2014, *A&A*, 572, A34
- Gastine, T., Yadav, R. K., Morin, J., Reiners, A., & Wicht, J. 2014, *MNRAS*, 438, L76
- Hall, J. C., & Lockwood, G. W. 2004, *ApJ*, 614, 942
- Hall, J. C., Lockwood, G. W., & Skiff, B. A. 2007a, *AJ*, 133, 862
- Hall, J. C., Henry, G. W., & Lockwood, G. W. 2007b, *AJ*, 133, 2206
- Houdek, G., Balmforth, N. J., Christensen-Dalsgaard, J., & Gough, D. O. 1999, *A&A*, 351, 582
- Isaacson, H., & Fischer, D. 2010, *ApJ*, 725, 875
- Karoff, C., Metcalfe, T. S., Chaplin, W. J., et al. 2013, *MNRAS*, 433, 3227
- Li, T. D., Bi, S. L., Liu, K., Tian, Z. J., & Shuai, G. Z. 2012, *A&A*, 546, A83
- Lockwood, G. W., Skiff, B. A., Henry, G. W., et al. 2007, *ApJS*, 171, 260
- Mamajek, E. E., & Hillenbrand, L. A. 2008, *ApJ*, 687, 1264
- Marcy, G. W., Isaacson, H., Howard, A. W., et al. 2014, *ApJS*, 210, 20
- Mathur, S., Metcalfe, T. S., Woitaszek, M., et al. 2012, *ApJ*, 749, 152
- Meibom, S., Barnes, S. A., Latham, D. W., et al. 2011, *ApJL*, 733, L9
- Meibom, S., Barnes, S. A., Platais, I., et al. 2015, *Nature*, 517, 589
- Metcalfe, T. S., Basu, S., Henry, T. J., et al. 2010, *ApJL*, 723, L213
- Metcalfe, T. S., Buccino, A. P., Brown, B. P., et al. 2013, *ApJL*, 763, L26
- Metcalfe, T. S., Creevey, O. L., Doğan, G., et al. 2014, *ApJS*, 214, 27
- Metcalfe, T. S., Creevey, O. L., & Davies, G. R. 2015, *ApJL*, 811, L37
- Nielsen, M. B., Schunker, H., Gizon, L., & Ball, W. H. 2015, *A&A*, 582, A10
- Oláh, K., Kővári, Z., Petrovay, K., et al. 2016, *A&A*, 590, A133
- Pace, G., Melendez, J., Pasquini, L., et al. 2009, *A&A*, 499, L9
- Petit, P., Dintrans, B., Solanki, S. K., et al. 2008, *MNRAS*, 388, 80
- Réville, V., Brun, A. S., Matt, S. P., Strugarek, A., & Pinto, R. F. 2015, *ApJ*, 798, 116
- Saar, S. H., & Brandenburg, A. 1999, *ApJ*, 524, 295
- Salabert, D., Régulo, C., García, R. A., et al. 2016, *A&A*, 589, A118
- Samadi, R., & Goupil, M.-J. 2001, *A&A*, 370, 136
- Shapiro, A. I., Solanki, S. K., Krivova, N. A., et al. 2014, *A&A*, 569, A38
- Skumanich, A. 1972, *ApJ*, 171, 565
- Valenti, J. A., & Fischer, D. A. 2005, *ApJS*, 159, 141
- van Saders, J. L., Ceillier, T., Metcalfe, T. S., et al. 2016, *Nature*, 529, 181
- Vaughan, A. H., & Preston, G. W. 1980, *PASP*, 92, 385
- Vidotto, A. A. 2016, *MNRAS*, 459, 1533
- Vorontsov, S. V., Christensen-Dalsgaard, J., Schou, J., Strakhov, V. N., & Thompson, M. J. 2002, *Science*, 296, 101
- Walker, G. A. H., Croll, B., Kuschnig, R., et al. 2007, *ApJ*, 659, 1611
- Wright, J. T., Marcy, G. W., Butler, R. P., & Vogt, S. S. 2004, *ApJS*, 152, 261